Mansoura Engineering Journal, (MEJ), Vol. 32, No. 2, June 2007. M. 13

AXIAL LOAD CAPACITY AND STRESSES IN COMBINED LOADED RADIAL BALL BEARINGS

قابلية التحميل المحوري والإجهادات في كراسي المحاور ذات الكريات المتدحرجة المحملة بأحمال مركبة

Elmidany, T.*, Hedia, H.**, Kohail, A.***, and Elkotb, M.****

* Prof. of Prod. Eng., Faculty of Engineering, Mansoura University, Egypt.
** Assoc. Prof., Faculty of Engineering, Mansoura University, Egypt.
*** Assoc. Prof., Specialized Studies Academy, Workers University, Egypt.
**** Asst. Lecturer, Specialized Studies Academy, Workers University, Egypt.

الملخص

يصف هذا البحث نموذج تفاعلي سهل الإستخدام لمحاكاة وتمثيل الحمل العمودي وزاوية التلامس والتشوه والإجهادات وذلك في اي موضع زاوي على مدار دورة كاملة وذلك لكراسي المحاور ذات الكريات المتدحرجة والمحملة بأحمال مركبة. تكمن اهمية هذا العمل في إمكانية تحديد زاوية التلامس والقوى العمودية المستحدثة من القوى المؤثرة وذلك في جميع المواضع للكريات المتدحرجة. يهدف هذا البحث إلى تقليل الإجهادات المؤثرة بين العناصر المتدحرجة ومساراتها في كراسي المحاور المتدحرجة والذي يهدف بدوره لاحقاً إلى إطالة العمر الافتراضي لهذه الكراسي، كما يخدم هذا البحث كلاً من مهندسي التصميم والصيانة.

Abstract

An interactive and easy to use simulation tool has been developed to simulate and depict normal loads, contact angle, normal deformations, and stresses at any angular position of the rolling element for combined loaded radial ball bearings. The importance of this work comes from the ability to determine the contact angle and induced normal load at any angular position. The main objective of this work is to lower stresses within the bearings, consequently, bearing fatigue life which is governed by stress level is significantly affected, showing that the lower the stress level the higher the service lifetime. This work is intended to serve both design and maintenance engineers.

Keywords: Ball bearings, Axial load, Bearing stresses, Contact angle.

1. Introduction

The operating characteristics of the rolling bearings depend greatly on the diametral clearance. Radial ball bearings are widely used in many diverse fields in industrial applications; they have advantages in high speed suitability and low frictional torque in comparison with cylindrical roller bearings. In this research, the principal geometrical

Accepted May 9, 2007

relationship governing the operation of radial ball bearings has been developed for both unloaded and loaded cases. Although radial ball bearings are designed to accommodate radial loads, they perform well under combined radial and thrust loads, they can also withstand misaligning loads of small magnitude. Axial load ability, axial play, and ability to misalign affected greatly by the amount of clearance within the bearing. The later is a function of the type of fit accomplished to mount the bearing and the differential expansion of the bearing components.

Analyses of load-stress relationships for rolling-element bearings were published by Lundberg and Palmgren [1]. These relationships were not easily usable until the analytical additions of Jones [2] led to the marketing of his computer code. Jones' code is still the most widely used rolling-element bearing analysis tool despite its age. Poplawski et al. [3] recently developed the code COBRA (Computer Optimized Ball and Roller Bearing Analysis).

2. Contact Angle

Radial bearings are generally designed to have diametral clearance in the no-load state. For this reason they have some axial play which implies a free contact angle different from zero. Fig. 1 shows a radial bearing with contact due to the axial shift of the inner and outer rings at no applied measurable force. The distance between the centers of curvature of the inner and outer ring races is

$$A = r_o + r_i - D \qquad (1)$$

The free contact angle [4], Fig. 1, is the angle made, in the unloaded bearing, by the line passing through the points of contact of the ball and both races and a plane perpendicular to the bearing axis of rotation. This angle can be expressed as

$$\alpha_f = \cos^{-1}\left(1 - \frac{P_d}{2A}\right) \qquad (2)$$

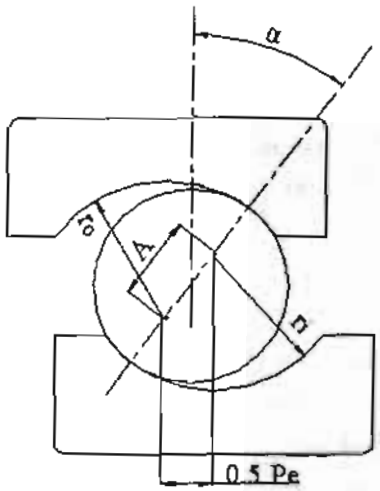

Fig. 1. Contact angle and endplay.

The free end play is defined as the maximum axial movement of the inner race with respect to the outer under no loads and expressed as

$$P_e = 2A\sin\alpha_f \qquad (3)$$

3. Misalignment Angle

Free angle of misalignment is the maximum angle through which the axis of the inner ring can be rotated with respect to the axis of the outer ring before stressing bearing components. It depends mainly on the

diametral clearance and the conformity, and described by Harris [5] as

$$\theta = 2\cos^{-1}\{1 - \frac{P_d}{4d_m}(\frac{(2f_o - 1)D - (P_d/4)}{d_m + (2f_i - 1)D - (P_d/2)} + \frac{(2f_o - 1)D - (P_d/4)}{d_m - (2f_o - 1)D + (P_d/2)})\} \quad (4)$$

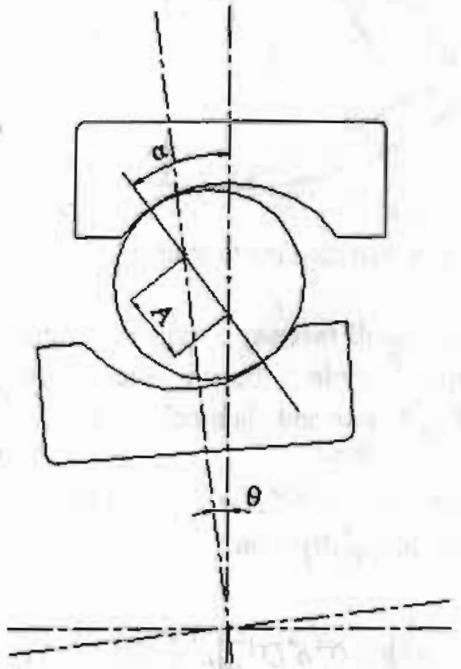

Fig. 2. Free angle of misalignment.

More simplified equation has been developed to represent the free angle of misalignment according to Fig. 2, hence

$$\theta = \sin^{-1}\left(\frac{A\sin\alpha_f}{d_i/2 + r_i}\right) \quad (5)$$

4. Clearance Reduction

Press fitting of the inner ring on the shaft causes the inner ring to expand slightly. Similarly, press fitting of the outer ring in the housing causes the former to shrink slightly. Thus, the bearing diametral clearance tends to decrease. Large amount of interference in fitting practices can cause bearing clearance to vanish and even produce negative clearance. Diametral clearance also affected by thermal conditions of bearing operation. Frictional moment within the bearing, and may be the environment, causes temperature rise and hence expansion of the bearing component, namely the shaft, and housing. Clearance tends to decrease or increase depending on the thermal gradient and the materials of the structure. The reduction in clearance due to interference fit and thermal expansion causes the diametral clearance to be diminished by the change in rings diameter and expansion of the bearing components, hence

$$\alpha_f = \cos^{-1}\left(1 - \frac{P_d + \Delta P_d}{2A}\right) \quad (6)$$

Where

$$\Delta P_d = \Delta_T - \Delta_s - \Delta_h \quad (7)$$

ΔP_d may have positive or negative values based on the amount of expansion in radial direction and the counter forces resist this expansion.

5. Stressed Contact Angle

When the bearing is subjected to only axial load, it exhibits an induced radial load which depends greatly on the contact angle, showing that, the lower the contact angle, the greater the induced radial load. The normal load to the contact area, Fig. 2, may be expressed as

$$Q_n = \frac{Q_a}{\sin\alpha} \qquad (8)$$

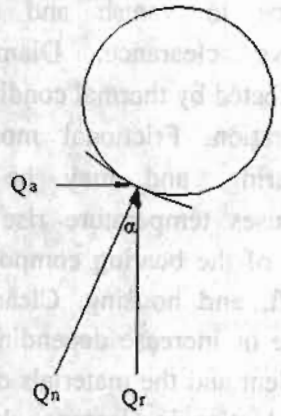

Fig. 3. Induced loads.

With the application of axial load, a stressed contact angle arises as shown in Fig. 3 beside the free contact angle expressed by Eq. (6). From Fig. 4 the stressed contact angle α_s can be expressed as

$$\cos\alpha_s = \frac{D/2-\delta}{D/2} = 1-\frac{2\delta}{D} \qquad (9)$$

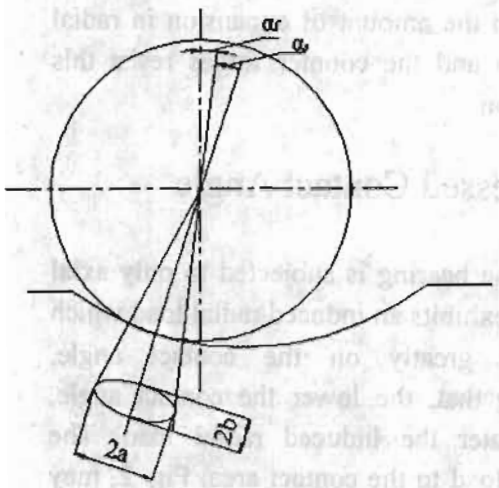

Fig. 4. Contact angle.

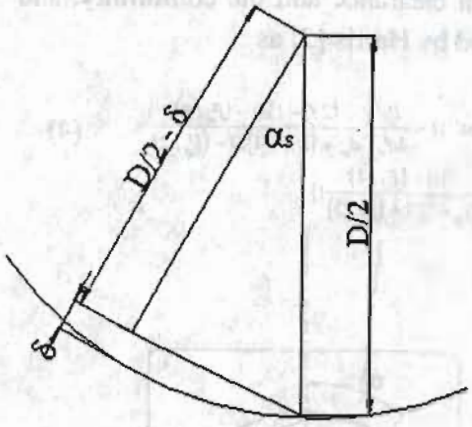

Fig. 5. Stressed contact angle.

For steel ball-raceway contact, the deformation within the contact was expressed by Brewe and Hamrock [6] as

$$\delta = 2.79\times10^{-4}\delta^{*}Q^{2/3}\Sigma\rho^{1/3} \qquad (10)$$

Substituting in Eq. (9), then

$$\cos\alpha_s = 1-5.58\times10^{-4}\delta^{*}D^{-1}\Sigma\rho^{1/3}\left(\frac{Q_a}{\sin\alpha_s}\right) \qquad (11)$$

This equation is to be solved by trial and error assuming different values for α_s until both sides of the equation are balanced for any other given data.

When the bearing is subjected to only axial load α_s expressed by Eq. (11) is considered constant at any angular location of the rolling element. With the application of radial load beside axial load, Q_r changes from zero to maximum according to rolling elements' angular location. Hence, for any angular location ψ, each rolling element is now subjected to axial load of constant value and different radial load. As a result, the

stressed contact angle α_s should be of different values depending on the rolling elements' location. When radial load per rolling element $Q_r = 0$, the stressed contact angle remains at maximum value determined from Eq. (11). As Q_r starts to increase, its induced axial load counteracts the original axial load Q_a increases and causes the stressed contact angle to decrease until they are of equal values causing the contact angle step-back to the free contact angle α_f. Extra increase in radial load will approximately vanish the contact angle to be of zero value.

The counteracting axial force induced by the application of radial load is expressed as

$$Q_{ia} = Q_r \sin\alpha \cos\alpha \qquad (12)$$

Where α is the total contact angle comprises the free and stressed contact angles

$$\alpha = \alpha_f + \alpha_s \qquad (13)$$

6. Normal Stresses

Applied axial and radial forces are transmitted normal to the contact area between the rolling element and raceways causing compressive stresses, which, should be within the elastic limits. Consequently, deformation in the form of small contact area develops. As these stresses depend mainly on the normal loads transmitted to the contact area, one of the main objectives of this research is to control these forces for optimal or at least better stressing.

The normal load induced by the application of only axial load is determined according to Eq. (8). When radial load starts to appear in combined loaded bearing, the equivalent load, Fig. 6, is determined as

$$Q_{eq} = \sqrt{Q_a^2 + Q_r^2} \qquad (14)$$

This equivalent load acts with an angle β to the radial load and its induced normal load can be determined as

$$Q_{n\psi} = \frac{Q_{eq\psi}}{\cos(\beta_\psi - \alpha_\psi)} \qquad (15)$$

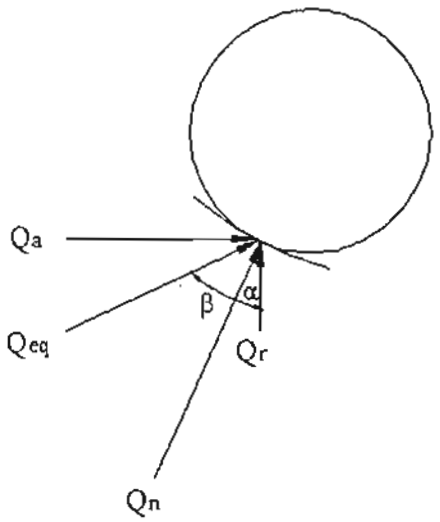

Fig. 6. Induced normal load.

For an elliptical contact area, the maximum compressive stress caused by the previously defined normal force occurs at the geometrical center. The magnitude of this stress is

$$\sigma = \frac{3Q_n}{2\pi ab} \qquad (16)$$

7. The Model

The mathematical description of building the bearing system model is very complex. The analysis of building the model is to be done by the dynamic model implementation in MATLAB-Simulink environment.

A model has been created based on the system of equations described in the previous sections. This model establishes the optimal load and stress distribution among the rolling elements and depicts relations between different diverse parameters for the simulated case. The model can be used for different cases with different parameters.

8. Case Study

To exhibit the power of the model, a case study with the specifications for the radial ball bearing 6209 mounted on solid shaft shown in Table 1 is cosidered.

Table 1 Bearing specifications

D_i	45 mm	r_o	6.6 mm
D_o	85 mm	P_d	0.015 mm
d_i	52.291 mm	F_r	4000 N
d_o	77.706 mm	F_a	2000 N
D	12.7 mm	Z	9
r_i	6.6 mm		

As the bearing subjected to both radial and thrust loads, both of them are transmitted normal to the contact area between the rolling element and raceways. When the rolling element is subjected to axial load, an induced normal load of higher magnitude arises, which depends greatly on the contact angle as depicted by the straight horizontal line in Fig. 7. This normal force starts to decrease with the appearance of radial load.

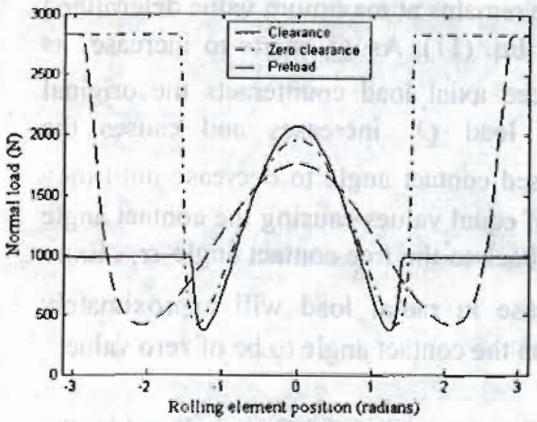

Fig. 7. Normal loads.

The contact angle depends greatly on the amount of radial clearance within the bearing and the position of the rolling element as can be shown in Fig. 8. With the increase of the contact angle, the axial load ability increases and hence, the normal load induced by the axial load decreases, Fig. 7.

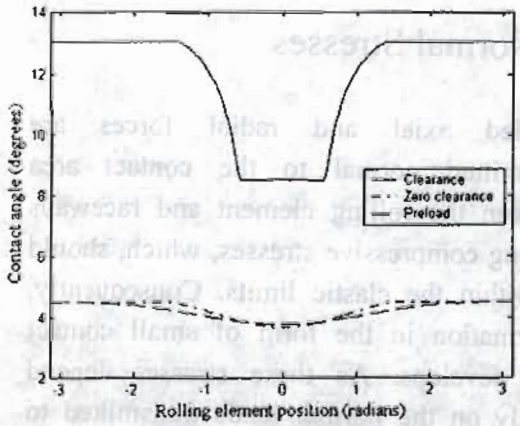

Fig. 8. Contact angles.

The normal deformation occurs between the rolling element and the raceways due to the

applied normal load is depicted in Fig. 9. These deformations are function of the applied load and the curvature of the raceway.

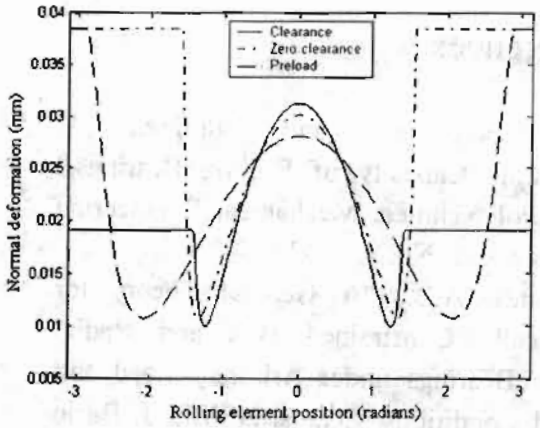

Fig. 9. Normal deformations.

Due to the normal load and deformation, a small elliptical area developed within the contact between the rolling element and the raceway. The maximum compressive stress occurs at the geometrical center of this area is depicted in Fig. 10.

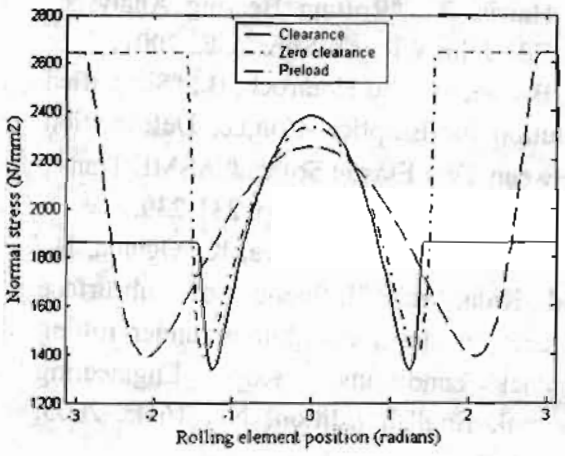

Fig. 10. Normal stresses.

9. Discussion

The ability of radial ball bearings to support axial loads depends mainly on the contact angle, where the later depends on the radial internal clearance within the bearing and the magnitude of the applied axial load. The case study was conducted to examine and depict the effect of radial internal clearance and different diverse parameters on the induced normal load, contact angle, deformation, and stresses at any angular position of the rolling element. Bearing failure due to subsurface defects will be of minimal magnitude as conducted by Yamakawa et al. [7].

Where bearing preload is favorable in most applications of radially loaded bearings, clearance is the most favorable for combined loaded radial bearings. With the clearance case, the contact angle increases, the induced normal load decreases, the deformation within the contact decreases, and finally the stresses are also decreased. The ability of radial ball bearings to support combined loads is better than supporting only axial loads as can be shown from the figures. This simulation tool clearly helps in selecting the optimal interference required to achieve the optimal performance.

10. Conclusion

A very useful and interactive simulation tool has been developed with which different cases with different parameters can be easily simulated for an optimal solution. This tool can be used successfully by maintenance engineers in fitting and maintenance

practices as well as design engineers in finding the recommended combination of radial and axial loads. The use of this tool helps in lowering stresses within the bearing which leads directly to increasing the bearing lifetime.

Nomenclature

Symbol	Description	Units
A	Distance between raceway groove curvature centers	mm
d_i	Inner raceway diameter	mm
d_m	Bearing mean diameter	mm
D	Rolling element diameter	mm
F	Force	N
f	r/D	
P_d	Bearing diametral clearance	mm
P_e	Free end play	mm
Q	Rolling element-raceway load	N
r	Raceway groove curvature radius	mm
Z	Number of rolling elements	
α_f	Free contact angle	°
α_x	Stressed contact angle	°
δ^*	Dimensionless parameter	
δ	Deformation	mm
Δ_h	Clearance reduction due to press fitting of bearing in housing	mm
Δ_s	Clearance reduction due to press fitting of bearing on shaft	mm
Δ_T	Clearance reduction due to thermal expansion	mm
θ	Misalignment angle	°
$\Sigma\rho$	Curvature sum	mm^{-1}
σ	Stress	N/mm^2

Subscripts

a	Refer to axial direction
i	Refer to inner raceway
n	Refer to normal direction
o	Refer to outer raceway
r	Refer to radial direction
ψ	Refer to angular location

References

1. Lundberg, G., and Palmgren, A. "Dynamic Capacity of Rolling Bearings," Acta Polytechnica, Mechanical Engineering Series, vol. 1, No. 3, 1947.

2. Jones, A.B., "A General Theory for Elastically Constrained Ball and Radial Roller Bearings under Arbitrary Load and Speed Conditions," Trans. ASME, J. Basic Eng., Vol. 82, No. 2, 1960, pp. 309–320.

3. Poplawski, J.V., Rumbarger, J.H., Peters, S.M., Flower, R., and Galaitis, H., "Advanced Analysis Package for High Speed Multi-Bearing Shaft Systems: COBRA," Final Report, NASA Contract NAS3–00018, 2002.

4. Hamrock, B., and Anderson, W., "Rolling-Element Bearings," NASA RP-1105, 1983, pp. 17-24.

5. Harris, T., "Rolling Bearing Analysis," 4th Ed., John Wiley & Sons, Inc., 2001.

6. Brewe, D., and Hamrock, B., "Simplified Solution for Elliptical-Contact Deformation Between Two Elastic Solids," ASME Trans., J. Lub. Tech. 101, 1977, pp. 231-239.

7. Yamakawa, K., Kizawa, K., Oguma, N., and Kida, K., "Influence of subsurface defects on stress distribution under rolling contact conditions," Koyo Engineering Journal, English Edition, No. 166E, 2005, pp. 24-28.